

PAPER • OPEN ACCESS

Aerotaxy: gas-phase epitaxy of quasi 1D nanostructures

To cite this article: Sudhakar Sivakumar *et al* 2021 *Nanotechnology* **32** 025605

View the [article online](#) for updates and enhancements.

Recent citations

- [Calculation of Hole Concentrations in Zn Doped GaAs Nanowires](#)
Jonas Johansson *et al*




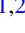







IOP | ebooks™

Bringing together innovative digital publishing with leading authors from the global scientific community.

Start exploring the collection—download the first chapter of every title for free.

Aerotaxy: gas-phase epitaxy of quasi 1D nanostructures

Sudhakar Sivakumar^{1,2} , Axel R Persson^{2,3,4} , Wondwosen Metaferia⁵ , Magnus Heurlin^{1,2} , Reine Wallenberg^{2,3,4} , Lars Samuelson^{1,2} , Knut Deppert^{1,2} , Jonas Johansson^{1,2}  and Martin H Magnusson^{1,2} 

¹ Solid State Physics, Lund University, Box 118, 221 00, Lund, Sweden

² NanoLund, Lund University, 22100, Lund, Sweden

³ Centre for Analysis and Synthesis, Lund University, Box 124, 22100, Lund, Sweden

⁴ National Center for High Resolution Electron Microscopy, Lund University, Box 124, 22100, Lund, Sweden

⁵ National Renewable Energy Laboratory, Golden, CO 80401, United States of America

E-mail: martin.magnusson@ftf.lth.se

Received 23 June 2020, revised 14 September 2020

Accepted for publication 28 September 2020

Published 14 October 2020



CrossMark

Abstract

Cost- and resource-efficient growth is necessary for many applications of semiconductor nanowires. We here present the design, operational details and theory behind Aerotaxy, a scalable alternative technology for producing quality crystalline nanowires at a remarkably high growth rate and throughput. Using size-controlled Au seed particles and organometallic precursors, Aerotaxy can produce nanowires with perfect crystallinity and controllable dimensions, and the method is suitable to meet industrial production requirements. In this report, we explain why Aerotaxy is an efficient method for fabricating semiconductor nanowires and explain the technical aspects of our custom-built Aerotaxy system. Investigations using SEM (scanning electron microscope), TEM (transmission electron microscope) and other characterization methods are used to support the claim that Aerotaxy is indeed a scalable method capable of producing nanowires with reproducible properties. We have investigated both binary and ternary III–V semiconductor material systems like GaAs and GaAsP. In addition, common aspects of Aerotaxy nanowires deduced from experimental observations are used to validate the Aerotaxy growth model, based on a computational flow dynamics (CFD) approach. We compare the experimental results with the model behaviour to better understand Aerotaxy growth.

Keywords: Aerotaxy, semiconductor nanowires, nanoscale synthesis

(Some figures may appear in colour only in the online journal)

1. Introduction

Over the past three decades, 1D nanostructures have attracted substantial interest due to their outstanding opto-electronic properties [1, 2]. They are expected to play a vital role both as

interconnects and as basic building blocks for future electronic and opto-electronic devices [3]. III–V compound semiconductors suited for multi-junction solar cells are expensive and have complex fabrication procedures [4]. Nanowire architecture is relatively more efficient in absorbing the incident light [5] and the nanoscopic dimension makes it possible to combine lattice-mismatched material and stack them on top of each other [6] at a fraction of the material consumption and production cost in comparison with traditional epitaxy. III–V nanowire ensemble devices are now a prime focus of research in next-generation, high-efficiency solar cells [7–9]. Reducing production costs and increasing the production volume makes



Original content from this work may be used under the terms of the [Creative Commons Attribution 4.0 licence](https://creativecommons.org/licenses/by/4.0/). Any further distribution of this work must maintain attribution to the author(s) and the title of the work, journal citation and DOI.

2. Aerotaxy technology

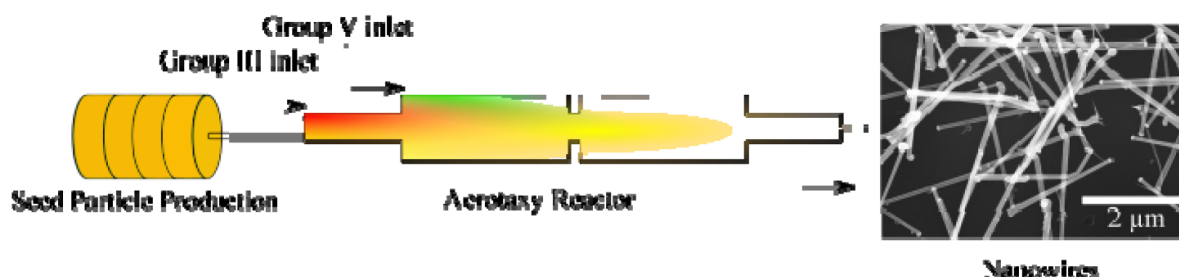


Figure 1. The principle of Aerotaxy. Catalytic particles (yellow) mix with gas-phase group III (red) and group V (green) precursors in a heated flow through the reactor to produce nanowires (SEM image).

III–V nanowires a viable alternative to current solar cell technologies. The most common method for nanowire fabrication is a ‘bottom-up’ approach that involves gold (Au) catalytic nanoparticles on a crystalline substrate, and the nanowires assemble layer by layer in an additive fashion on the substrate. The catalytic nanoparticles in the presence of suitable precursors enhance growth in one dimension producing 1D nanostructures [10]. Depending on the capability of the growth technology used, nanowires with precise dimensions, crystallinity and materials composition [11] can be manufactured. metal organic vapor phase epitaxy (MOVPE) is a bottom-up approach that has been used for manufacturing semiconductor nanowires since the early 1990s [12] and can fabricate nanoscale structures with surface quality on par with molecular beam epitaxy (MBE). Both methods suffer in throughput from batch processing and demand expensive crystalline substrates, increasing the overall production cost [13]. Though cheaper alternatives exist for nanowire production [14], they often suffer from poor material quality or the wires lack in the beneficial optoelectronic properties that make the nanowire architecture interesting.

In order for nanowires to become key semiconductor building blocks, a cost efficient and high throughput production method is crucial. Aerotaxy [15] is a growth technology that serves the purpose of producing nanowires continuously without a crystalline substrate. Size-selected catalytic Au nanoparticles mix with III–V precursor flux in a hot flow-through reactor. Rapid growth occurs at a rate of $\sim 1 \mu\text{m s}^{-1}$ [16] and the resulting nanowires can be collected on substrates/filter for further processing. The Aerotaxy technique avoids the need for pre-patterned, crystalline substrates and can be operated continuously with high throughput. Scalability is in general easier for continuous bulk chemical reaction processes as compared to batch-based surface processes like MOVPE. Scaling can be done by increasing e.g. reactor volume or carrier gas velocity, or by parallelization of sub-processes. In this paper, we describe our modular system, present the Aerotaxy growth process in detail and provide an explanation of the principal theory behind it.

Systematic understanding of nanowire crystal growth is necessary in order to exploit the useful electro-optical properties of nanowires. R S Wagner and W C Ellis from

Bell laboratories [17] proposed the vapor–liquid–solid (VLS) growth model in 1964 to explain sub-mm Si wire growth. They proposed that the liquid Au droplet on the substrate acts as a sink or enhances cracking of the precursors in the vapor phase that subsequently precipitates into the solid crystal phase. The most common steps in VLS wire growth consist of (i) preparation of catalyst nanoparticles by aerosol deposition or lithography, (ii) heating the substrate along with catalyst particles to form liquid alloy droplets that can aid in nucleation, and (iii) supplying gaseous precursors that precipitate into the solid crystal phase [18]. Today the VLS mechanism is the most commonly employed route to achieve nanowire growth. There is also a relatively less common vapor–solid–solid (VSS) mechanism [19] in which growth occurs from a solid catalyst particle below its eutectic melting point. Our experiments in Aerotaxy were performed at temperatures above this eutectic point for both binary and ternary semiconductor systems, and the maximum growth rate we observed is much higher than that predicted by VSS, hence we adopt the VLS framework to understand nanowire growth.

2. Aerotaxy technology

The earliest mention [20] of Aerotaxy in literature reports on direct conversion of Ga nanoparticles to crystalline GaAs in a hot H_2 atmosphere containing arsine (AsH_3). This gas-phase approach was later used for making elongated InP particles [21]. Eventually, Aerotaxy was extended to produce crystalline nanowires in a tube furnace by mixing metalorganic (MO) precursors to the gas phase [16]. Gold nanoparticles catalysed the growth of nanowires in a continuous flow-through reactor assembly as shown in figure 1. Au nanoparticles are produced commonly by following methods (i) chemically reducing a solution containing gold to precipitate metallic gold nanoparticles [22, 23] (ii) laser ablation [24], solvothermal synthesis [25] (iii) electrochemical synthesis [26]. Most of these techniques produce Au nanoparticles as liquid suspensions; however, it is not simple to extract the nanoparticles from a liquid and disperse them into the gas phase to aid Aerotaxy growth. Direct production of Au particles by aerosol methods (see process details below) is therefore used [27].

Conventional VLS growth of III–V nanowires occurs through surface diffusion of precursor adatoms on the substrate and through direct impingement of adatoms on the seed particle [28]. In Aerotaxy however, there is no substrate for adatom migration. Our current understanding is that Aerotaxy growth (for our standard GaAs nanowires) initiates when Au nanoparticles are mixed with Ga precursor at a suitable temperature at which Ga forms an alloy with the seed particle. When the Au–Ga alloy particle is subsequently exposed to AsH₃, As atoms begin to dissolve in the particle, which effectively becomes supersaturated with (Ga, As), which can precipitate as solid GaAs. In VLS nanowire growth, a seed particle contains enough excess (Ga, As) to grow at most a couple monolayers of GaAs (for very small particles less than one layer) before attaining equilibrium. In Aerotaxy, homogeneous nucleation initiates growth (in the absence of a particle–substrate interface), requiring a higher degree of supersaturation. We thus expect it to yield an initial crystallite with a somewhat larger volume than that of a few monolayers of planar growth, and it will likely form on the surface of the Au–Ga particle. A continuous supply of As (and Ga from the remaining TMGa) from the gas phase quickly make the particle supersaturated again, and the next nucleation event will most likely happen somewhere adjacent to the first crystallite, and also at the surface of the particle. Since the partial pressures of the precursors in Aerotaxy is ~ 100 times higher in comparison with MOVPE, the next nucleation happens with a very short delay, and will likely form a crystal that is not perfectly aligned with the first one. Thus, multiple nucleation events create a cluster of GaAs crystallites, which is soon the same size as the seed particle, and surface tension will make the particle stick to one side of the growing GaAs cluster. Some nucleation events will lead to growth of crystalline grains, where fast-growing surfaces taper into points (since growth at corners is not favored), according to the kinetic Wulff plot, which has been discussed for GaN nanostructures by Jindal and Shahedipour-Sandvik [29]. Alternatively, the surfaces meet the edge of the seed particle and cannot continue growing. Eventually this will leave only a single (111)B surface extending across the width of the now approximately hemispherical seed particle. Once the slow-growing [111]B direction is established, subsequent growth proceeds further by adding new planes in the [111]B direction; the preferred directionality has been demonstrated by TEM [16]. At this point, growth continues more or less in the same way as in conventional nanowire growth, except that there is no substrate to supply group-III material. We do acknowledge that this hypothesis is qualitative and difficult to verify experimentally. Intrinsic directionality of Aerotaxy wires similar to substrate-assisted nanowires allows the possibility to fabricate nanowires with excellent crystallinity. To the best of our theoretical and experimental understanding, the common aspects of Aerotaxy-grown nanowires are:

- The wires have a base filled with dense stacking faults under all investigated growth conditions, and the size of this base appears to vary randomly.
- High Resolution Transmission Electron Microscopy (HR-TEM) investigations show that the nanowires prefer to grow with zincblende structure in the [111]B direction with stacking faults in the 111 planes.
- Average nanowire length is largely insensitive to variations in seed particle diameter.
- The average length is also largely insensitive to variations in precursor flows (figures 4(a)–(f)).
- High precursor fluxes usually invoke parasitic growth, dust etc (figures 4(a)–(f)).
- The average nanowire length is measured to be within 2–3 μm in the current reactor configuration. Statistical treatment of the length measurements at a particular growth condition leads to a smaller range with a mean standard deviation of $\pm 15\%$.
- Higher growth temperature produces longer and more tapered wires.

In Aerotaxy, metallic gold is evaporated in a high-temperature (HT) furnace maintained at a temperature between 1800 °C and 1900 °C and the condensed vapor is size-selected with the help of a differential mobility analyser (DMA) to produce Au nanoparticles [27, 30]. Nitrogen carrier gas flows through the HT furnace at a rate of 1.5 l min⁻¹ carrying the Au vapor into the radiation charger and then to the sintering furnace. The Au particle concentration in the aerosol can be modulated with HT furnace temperature or carrier gas flow as they directly affect the rate at which the Au evaporates. The smaller sintering furnace is heated to a temperature of 550 °C at which the agglomerates partially melt and compact to a roughly spherical shape [31]. The DMA helps to achieve a narrow size distribution of charged nanoparticles based on their aerodynamic size, which in our system is tunable between 10 nm and 100 nm. Catalytic particle-size is one of the user-defined parameters in Aerotaxy used for tuning the optical and electrical properties of the nanowires [32, 33]. Appropriate mass flow controllers (MFCs) regulate all gas flows through the system. An electrometer downstream continuously monitors the flow of the aerosol.

This Aerotaxy tool was designed and built in close collaboration with the start-up company Sol Voltaics AB, which has also built up-scaled versions based on the same principle [34, 35]. The reactor (figure 2) is built from stainless steel tubes, with ultra-high vacuum joint seals. Resistive coils in a three-zone clamshell furnace surrounds the reactor. In the case of GaAs wire growth, size selected Au aerosol is mixed with trimethylgallium (TMGa) diluted in nitrogen carrier gas in the alloying zone of the Aerotaxy reactor, maintained at around 430 °C. The aerosol is at room temperature before reaching the reactor. The steep temperature profile of the alloying zone in the presence of Au nanoparticles under near atmospheric pressure allows a fraction of the Ga precursor to decompose and alloy with the Au particle. The Au–Ga particles are carried further downstream into the growth zone, maintained at a higher temperature relative to the alloying zone, typically around 550 °C. As shown in figure 2, the flow downstream enters a wider volume of the growth zone. The active flow

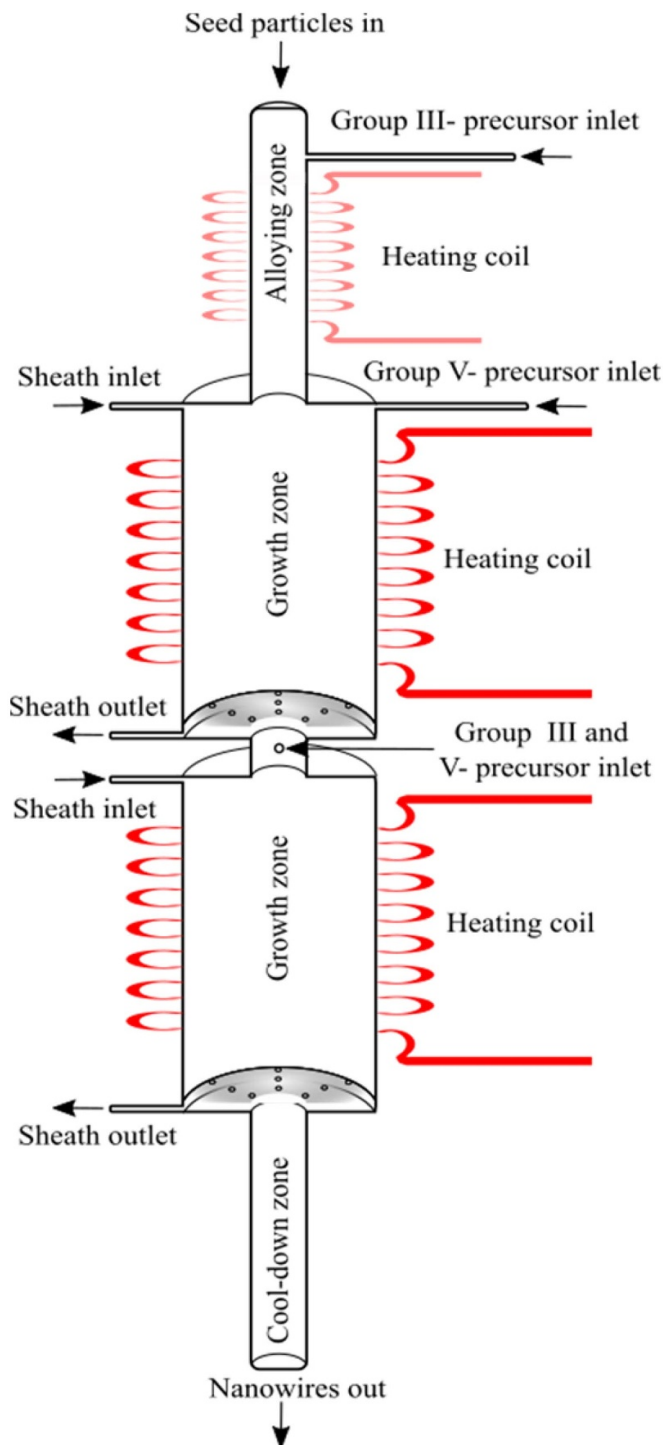


Figure 2. Schematic of the Aerotaxy reactor, drawn approximately to scale; the heated zones have a total height of 750 mm. Au aerosol particles enter the reactor at the top through the alloying zone, travels down into the growth zone to mix with group III and V precursors, producing nanowires that exit from the cooling zone. Sheath gas enters and exits both growth zones through showerhead diffusers that ensure laminar flow. The gas transit time from top to bottom is around 6 s for standard flow and temperature settings.

in the growth zone is surrounded by a sheath gas flow acting as a buffer between the reactor wall and the aerosol. The alloyed particles are thus heated further in an arsine (AsH_3)

atmosphere in the growth zone. Preferential 1D growth occurs at a rapid rate of $\sim 1 \mu\text{m s}^{-1}$, forming crystalline nanowires on the Au nanoparticles during the time spent in the growth zone. The total growth time is ~ 3 s and is dictated by the residence time in the heated zones of the tube furnace and can be modulated by adjusting the flow rates. Approximately 300 million atoms (for our standard GaAs nanowires) find their position within the crystal lattice of each nanowire at a rate of ~ 120 million atoms per second. The nanowires along with the residual precursors are carried down into the cooling zone maintained at ~ 130 °C. The cooling zone avoids turbulent mixing in the lower growth zone by gradually reducing the temperature of the gas phase. As the aerosol exits the reactor, the gas cools down to room temperature and flows to a deposition chamber for collection onto a suitable substrate/filter. The deposition chamber consists of a single stage, circular-plate, dry electrostatic precipitator (ESP) placed perpendicular to the gas flow. In practice, a Si wafer or a TEM grid is placed on the ESP to collect the incoming nanowires. The ESP collects the wires from gas phase by applying a high voltage to the circular collection plate [36]. The nanowires retain the charge carried by the Au seed particles, so the ESP can easily filter them out. The residual gases, along with uncollected wires, are pumped out from the system through particle filters and a gas scrubber. All outgoing gas flows are controlled by low Δp MFCs.

Instead of on a substrate, the nanowires can also be collected on a filter with a pore size smaller than the nanowire's aerodynamic size. The collected nanowires land randomly on the substrate/filter. Randomly oriented nanowires may appear counterintuitive to our goal, as ensemble nanowire devices are rarely built from random clusters. But, photoconductors made from ensemble of randomly oriented InP nanowires on hydrogenated silicon film exploits the randomness to geometrically trap the incident radiation [37]. The same geometrical light trapping phenomena can also be used for anti-reflection purposes. Randomly oriented silicon core-shell nanowires act as graded index broadband and wide angle antireflection coating for next generation photovoltaics [38]. Randomness in orientation thus seems to be useful to some aspects of next generation nanowire devices. However, when it comes to devices beyond proof of concept, most nanowire ensemble devices strictly require suitably aligned nanowires. Large-area alignment of nanowires from colloidal solutions grown by Aerotaxy has indeed been demonstrated by our industrial partner [39].

The Aerotaxy reactor is designed for mass-producing semiconductor nanostructures with uniform dimensions and high crystallinity. A layer of N_2 gas flow separating the reactant flow from the wall is established through sheath inlets at the top and outlets at the bottom of both the growth zones. The wire length strongly depends on the residence time inside the reactor. Operating in the laminar flow regime helps to avoid wide variations in residence time, especially within the growth zones, and in turn helps to achieve a narrow distribution in wire length. In laminar flow regime, the velocity profile of gas inside a circular pipe is a parabola with its fastest moving layers at the centre and the slowest layers near the inner pipe walls. Such disparities in the velocity profile would lead to non-uniform residence times within the growth zone, which

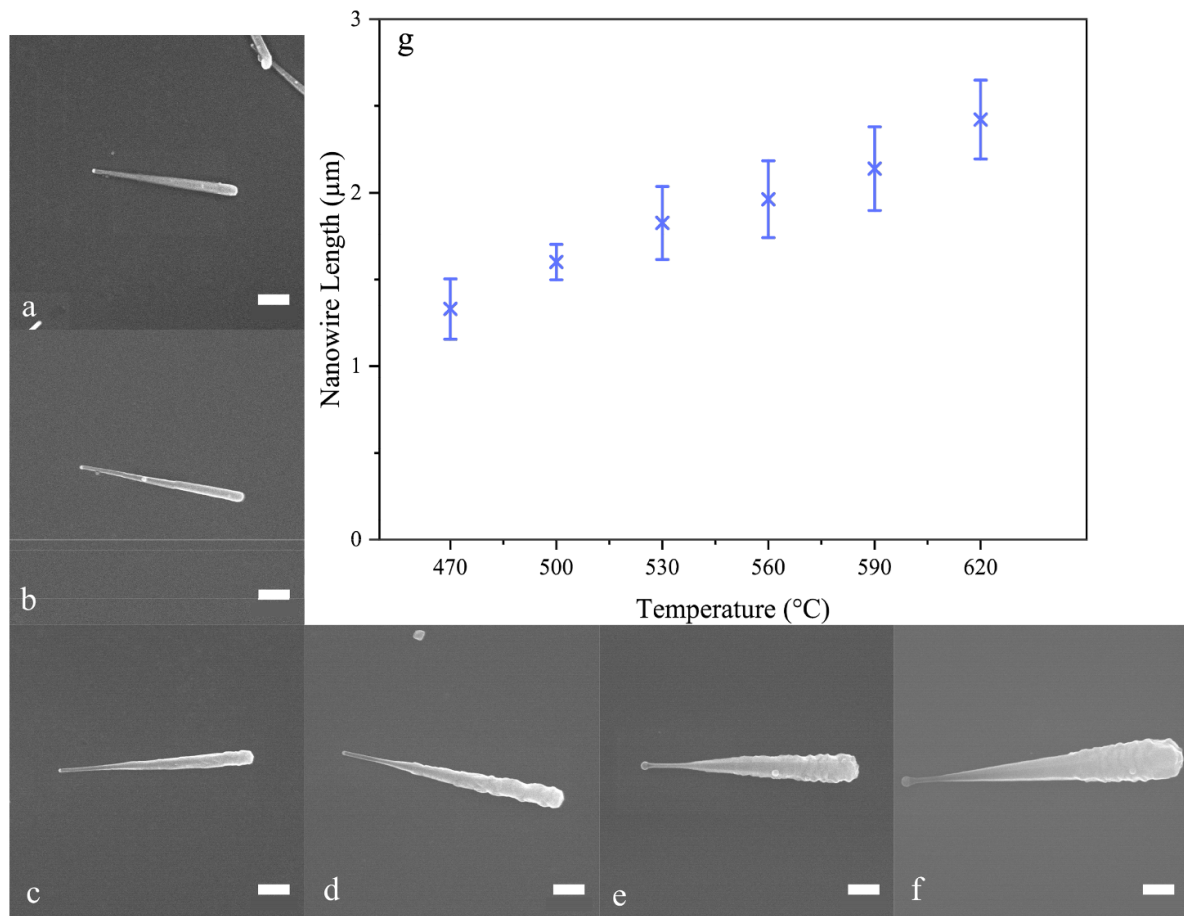


Figure 3. SEM images of GaAs nanowires grown from 30 nm Au particles at reactor furnace set points of (a) 470 °C (b) 500 °C (c) 530 °C (d) 560 °C (e) 590 °C (f) 620 °C, and at a V/III ratio of 1.6. (g) Temperature dependence of the nanowire length (error bars: std. of measured nanowire length based on 10–20 manual measurements). Scale bars: 300 nm.

will inevitably affect the wire-length distribution. This is one of the reasons for using a sheath gas flow, as it effectively filters the slowest parts of the gas and promotes a near uniform velocity profile. Apart from that, the sheath flow adds a buffer layer of gas between the growing wires and the reactor wall. Early growth observations showed that wall interaction leads to parasitic growth, which in turn leads to loss of wire production.

In our configuration, the precursor injectors are placed at different zones along the reactor to separate the supply of group III and V precursors. Separation of precursors until the reaction surface is a commonly employed tactic in MOVPE to avoid stray reactions among the precursors resulting in unwanted effects. However, in Aerotaxy the reaction surface is not present during the initial stages but is fabricated during nucleation. Therefore, systematic separation of reactive species until the reaction surface assembles is paramount for proper nucleation and subsequent wire growth. Reactive species that mix in the absence of alloyed Au–Ga seed particles produce III–V dust instead of nanowires. Group III precursor flux and Au seed particles mixed in the first zone also allows for efficient alloying of the seed particle. Aerotaxy nanowires with core–shell structures or *pn*-junctions [35] have been demonstrated by adding consecutive growth

chambers in series. In our reactor, the growth zones consist of two reaction chambers with identical dimensions. The second growth chamber separated from the first by a short tube, allows injection of additional precursors, such as group III, V and dopant precursors, allowing growth of shells, *pn*-junctions or heterostructures. In theory, two reactors in separate furnaces could be connected in series to achieve this. This was indeed tested in a previous version of the Aerotaxy system, but observations showed that in this configuration most of the nanowires became kinked or malformed, since a constant temperature between the growth zones was not maintained.

3. Growth results and discussion

The first paper on Aerotaxy-grown GaAs nanowires [16] reported that nanowire length increased with growth temperature. This initial work was done in a much simpler configuration, essentially just precursors mixed with an aerosol sent through a heated ceramic tube. Subsequent publications [40, 41] were made using the system described in this paper. We here present further results from growth in this system.

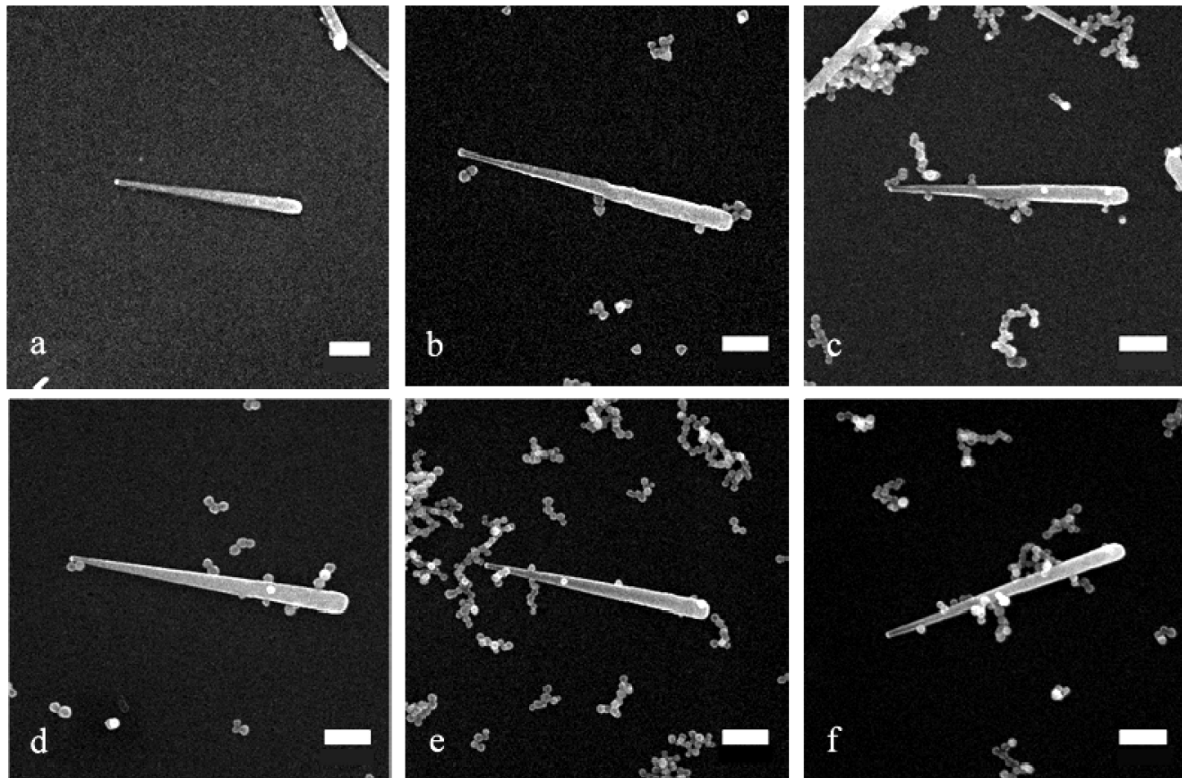


Figure 4. SEM image of GaAs nanowires grown from 30 nm Au particles at V/III ratio of (a) 1.6 (b) 1.8 (c) 2.0 (d) 2.2 (e) 2.4 (f) 2.6 and at a reactor furnace set point of 530 °C. It is evident from the SEM images that parasitic particle density increases with increasing V/III ratio while the wire length remains unaffected. Scale bars: 300 nm.

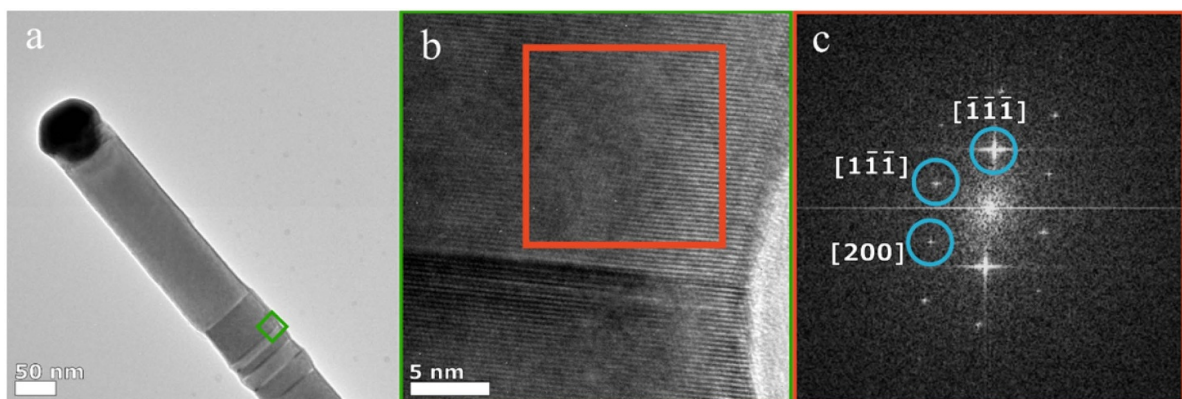


Figure 5. (a) A TEM image of GaAs nanowire. (b) shows a higher magnification image (HR-TEM) of the region highlighted by green square in (a) and (c) shows an FFT of the highlighted red square in (b) confirming the wire has zincblende-structure.

There is a complex dependence between nanowire morphology, length, crystal structure and growth temperature in Aerotaxy. Parasitic reactions between TMGa and AsH₃ are enhanced at high growth temperatures, thus producing Ga- and As-containing dust. The axial growth rate of the nanowire increases with the growth temperature (figure 3(g)), and nanowires grown at higher temperatures become more tapered, as shown in figures 3(a)–(f). A higher growth temperature could also lead to increased desorption of precursors, which could in turn lead to a shorter diffusion length along

the sidewalls. In comparable epitaxial techniques, the axial growth rate is suppressed at high temperatures due to parasitic thin film growth on the substrate. Eliminating the substrate in Aerotaxy enables us to achieve successful nanowire growth over a wider temperature window.

Aerotaxy growth is reported to prefer a low V/III ratio [16] as it helps with saturating the Au droplet with group III species. Aerotaxy wires are typically free from parasitic particles at the lowest V/III ratios (figure 4(a)) but the parasitic particle density clearly increases with increasing V/III ratios. A high V/III

ratio favors formation of parasitic particles without inhibiting the underlying nanowire growth (figures 4(c)–(f)). Due to lack of a substrate, adatom migration occurs by direct material influx through the catalytic particle and diffusion of adatoms along the nanowire surface. An increase in material influx at high precursor flows reduces the diffusion length of the adatoms that contribute to wire growth. The additional material flux also contributes to parasitic reactions and may lead to formation of nanoparticles present along with wires. TEM-based x-ray energy dispersive spectroscopy (XEDS) studies on Sn-doped GaAs nanowires revealed that the parasitic particles were made either of GaAs or Ga crystals [41, 42]. Particle composition for other material systems has not been tested so far.

Polytypism is a common occurrence among VLS III–V semiconductor nanowires [43]. Aerotaxy-grown nanowires [16, 40, 44] are found to exist in pure zincblende phase (figures 5(b), (c)) at low (lowest temperature with successful wire growth) to moderately high growth temperatures. At even higher growth temperatures, the nanowires are found to exist intermixed with wurtzite sections between zincblende phases; this was first reported in [16], but is also present in wires grown in the subsequent complex Aerotaxy systems. HR-TEM investigations show that all investigated wires have a base filled with dense stacking faults and that growth occurs in the [111]B direction.

GaAsP nanowires with tuneable bandgap have been successfully grown with Aerotaxy by using a mixture of arsine and phosphine as group V source [40]. Au catalysed III–V ternary nanowire growth is relatively less understood, since existing VLS models based on surface energies, chemical potentials and diffusivity fall short when explaining wire growth in ternary systems like GaAsP [28]. Similar to MOVPE grown GaAsP nanowires, the P content of Aerotaxy wires varies non-linearly with the gas phase P ratio [40, 45]. The bandgap energy of Aerotaxy GaAsP nanowires is modulated by the gas phase ratio of group V precursors by altering the P content in the wire. HR-TEM investigations revealed GaAsP wires exist in pure zincblende phase with twin plane defects even at higher growth temperature.

Successful *n*- and *p*- doping of GaAs has previously been reported using tetraethyltin (TESn) [41] and diethylzinc (DEZn) [44] respectively introduced with the TMGa in the alloying zone. It was observed that *in situ* doping has little to no effect on the nanowire growth rate. However, at high dopant injection ratios (dopant/TMGa), the morphology of the nanowires suffered from high incidence of parasitic growth at the base, whereas low dopant injection ratios gave morphologically superior nanowires with less tapering. TEM investigations [42] proved that the doped nanowires still preferred the [111]B growth direction with zincblende crystal structure. Dopant content in the alloyed seed particle seemed to drive the dopant incorporation into the nanowire for both *n*- and *p*-doped GaAs. We consistently observe doping levels above $5 \times 10^{18} \text{ cm}^{-3}$. Recent thermodynamic modelling suggests that it is very hard to reliably achieve medium or low Zn doping in VLS growth, including Aerotaxy [46].

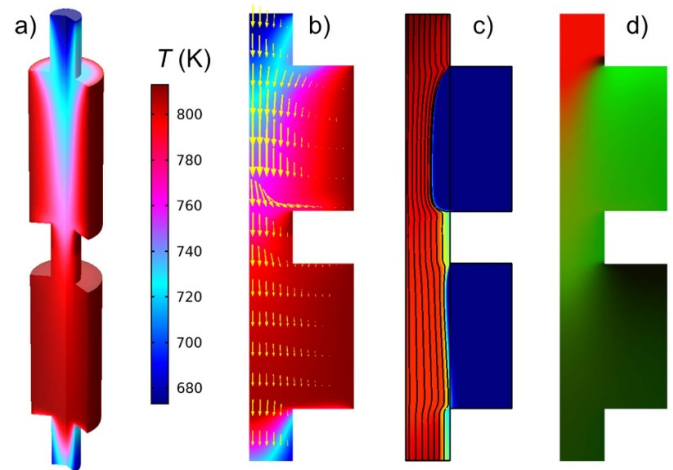


Figure 6. (a) the rotated 2D geometry in proportional scale of the gas volume where nanowire growth occurs. The total length of the reactor volume modelled here is 450 mm and the diameter is 55 mm; (b) temperature (color scale) and gas flow (arrows); (c) Au seed particles following the core flow; and (d) the convective/diffusive transport of TMGa (red) and AsH₃ (green). Images (b)–(d) are radial cross sections with exaggerated radial scale.

4. Wire growth and process modelling

The Aerotaxy process takes place inside a stainless steel cylinder heated by a tube furnace. This design is suitable for creating a controlled gas flow structure but makes it very difficult to introduce view- or sampling ports without disturbing the process and risking dangerous leaks. Therefore, modelling is the best option for better understanding how the growth process works. This modelling is based on computational flow dynamics (CFD) and chemical reactions based on a growth model for individual wires.

To account for the qualitative growth observations above, in particular that the wire length depends only weakly on seed particle diameter and precursor partial pressures, a new model for nanowire growth was needed. Previous models [47, 48] describing nanowire growth exhibit the opposite behaviour, being developed for very different growth systems, where the precursor pressures in MOVPE commonly are on the order of 10^{-3} mbar, at least for the group III precursors, and much lower than this in MBE. In Aerotaxy, the precursor pressures of both group III and V are about one mbar.

The new growth model is described in detail by Johansson and Magnusson [49] and is summarized by the following relation for the wire growth rate G :

$$G = \Omega I \frac{J_3 \varphi}{J_3 \varphi \left(1 + \frac{k_d}{J_5}\right) + I} \quad (1)$$

where Ω is the molar volume of a III–V dimer, I is the rate limiting incorporation factor, J_i is the impingement rate of precursor species i , k_d is the desorption rate of group V atoms, and $\varphi = 2(1 + \lambda/R)$ is a shape factor with R being the seed particle radius and λ either the diffusion length or the wire length, whichever is shorter. For high precursor pressures, the

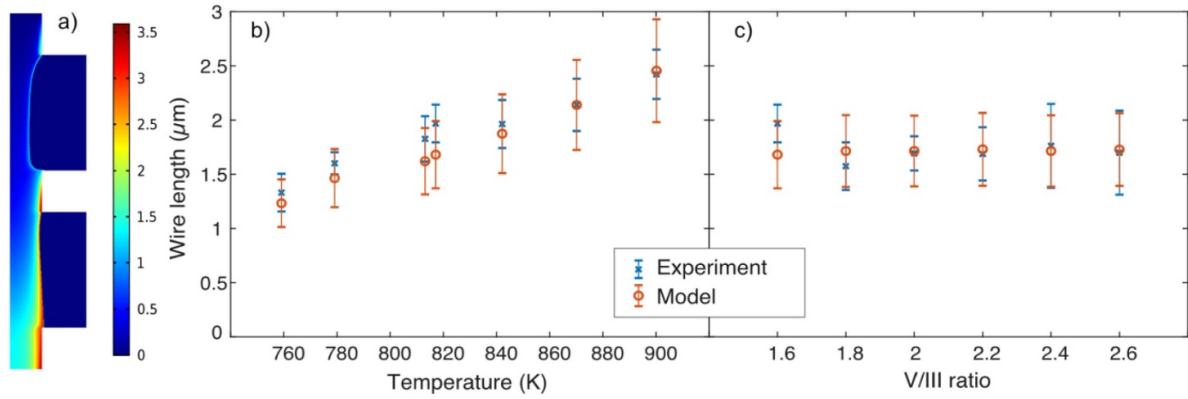


Figure 7. (a) plot of the wire length L_{NW} during steady-state growth in the reactor. (b) Wire length as a function of peak temperature for GaAs nanowires grown at a fixed V/III ratio of 1.6. (c) Length as a function of V/III ratio for nanowires grown at a peak temperature of 815 K (set point 530 °C). In both plots, the model is shown as red rings and the experiment as blue crosses, with the error bars indicating plus/minus one standard deviation.

growth rate reduces to simply $G = \Omega I$, i.e. independent of flows and radius, in agreement with the growth observations. The incorporation rate is assumed to be thermally activated with $I = k_r e^{-E_r/kT}$.

The Aerotaxy process modelling will be described in more detail in a coming paper; here we give only a summary of the results. We start with a CFD model of the growth reactor, realized in COMSOL Multiphysics® [50] in a rotated cylindrical 2D geometry, cf figure 6(a). Only the gas volume is included in the model: gas flows in and out of the reactor (as shown in figure 2 above) are measured with MFCs and the temperature profile at the outer surface is set by measurements at eight points along the reactor; the temperatures used for modelling are presented in K. The ‘growth’ temperature used in figure 7 is defined as the peak temperature in the reactor, which is up to 12 K higher than then the furnace set point. Figure 6(b) shows the resulting temperature and flow pattern. Once the flow and temperature profiles are calculated, Au seed particles are introduced in the core flow as a gas with very low diffusion coefficient, to simulate particles. In figure 6(c), the Au particle concentration c_{Au} is visualized in red, showing that they follow the gas streamlines and are confined to the core flow by the two sheath flows and is close to a step function in the radial direction. And in figure 6(d), the interdiffusion of TMGa and AsH₃ is visualized using red and green overlay, where yellow tone indicates a mixture of the two precursors.

Nanowire growth is then modelled at steady state using the full expression (equation (1)), not using the high flow limit. Wire growth (here GaAs) occurs only in the presence of the Au seed particles and GaAs is modelled as a gas with the same low diffusion coefficient as the particles. Wire length at each point in the reactor is calculated by dividing the concentration of GaAs with that of Au, using the particle cross section area and molar volume to get the units right. The wire length is set to zero where the Au concentration is very low, to avoid division by zero. The diffusion length λ is set to 1 μm based on TEM observations, group V desorption k_d is set to zero and only the incorporation rate activation energy E_r and prefactor k_r are used as fitting parameters.

Figure 7(a) shows the wire length L_{NW} at each point. The resulting average length of the wires \bar{L} is calculated by a line integral along the reactor exit:

$$\bar{L} = \frac{\int u_z c_{Au} L_{NW} r dr}{\int u_z c_{Au} r dr} \quad (2)$$

where u_z is the downward flow out of the reactor. The standard deviation of the wire length is calculated in a similar fashion. Both the wire length average and variation are used to determine the fitting parameters.

This model behaves qualitatively as intended, with the resulting average wire length unaffected by the seed particle size, and only weakly depending on the precursor flow. Figure 7 shows a comparison between modelling and experiment for different peak temperatures (b) and V/III ratios (c), with good agreement in both average length and standard deviation. In this experiment, the TMGa pressure range was 62–70 Pa and the AsH₃ pressure range was 99–112 Pa. The nominal diameter of the gold particles was 30 nm. In the model, the activation energy for nanowire growth is 38 kJ mol⁻¹ based on an Arrhenius plot of the length and temperature data.

5. Conclusions

In summary, we have provided an overview of the low-cost, high throughput, continuous Aerotaxy nanowire growth process. We have discussed in detail about the technical aspects of our custom-built Aerotaxy system. The morphology and dimensions of the nanowires exhibit a tangible dependence on factors like growth temperature, time and precursor flux ratios. This observation is in agreement with previous studies conducted with Aerotaxy. The nanowires discussed here exhibit an inherent directionality even when grown in gas phase and prefer to exist in zincblende crystal structure. Exploration of the growth parameter space has helped us to achieve well-defined boundaries between wire and parasitic growth.

The CFD Aerotaxy model shows a good agreement with our experimental observations, such as the temperature

dependence of nanowire length, the insensitivity to seed particle diameter and precursor flows. The model is however not yet capable of showing the origin of the crystal structure observations and the occurrence of high density stacking faults at the base in Aerotaxy wires. Further experiments are required to reinforce our CFD model to improve its predictive capabilities and model the effect of doping.

Acknowledgments

This work was performed in Lund Nano Lab within the MyFab cleanroom infrastructure and with financial support from NanoLund, the Swedish Research Council, the Swedish Energy Agency, the European Union's Horizon 2020 research and innovation programme under Grant Agreement 641023, the Crafoord foundation, and from the Knut and Alice Wallenberg Foundation. We acknowledge Bengt Mueller and the Aerotaxy team at Sol Voltaics AB, especially Linda Johansson and Greg Alcott, for technical support and discussions.

ORCID iDs

Sudhakar Sivakumar  <https://orcid.org/0000-0002-0205-9036>

Axel R Persson  <https://orcid.org/0000-0002-0399-8369>
Wondwosen Metaferia  <https://orcid.org/0000-0003-1581-830X>

Reine Wallenberg  <https://orcid.org/0000-0002-0850-0398>

Lars Samuelson  <https://orcid.org/0000-0003-1971-9894>

Knut Deppert  <https://orcid.org/0000-0002-0471-951X>

Jonas Johansson  <https://orcid.org/0000-0002-2730-7550>

Martin H Magnusson  <https://orcid.org/0000-0002-8049-2142>

References

- [1] Ramanujam J, Shiri D and Verma A 2011 Silicon nanowire growth and properties: a review *Mater. Express* **1** 105–26
- [2] Puglisi R A, Lombardo V and Caccamo S 2017 Silicon quasi-one-dimensional nanostructures for photovoltaic applications *Nanowires—New Insights* (Rijeka: InTech) pp 131–53
- [3] Kuchibhatla S V N T, Karakoti A S, Bera D and Seal S 2007 One dimensional nanostructured materials *Prog. Mater. Sci.* **52** 699–913
- [4] Dimroth F et al 2014 Wafer bonded four-junction GaInP/GaAs/GaInAsP/GaInAs concentrator solar cells with 44.7% efficiency *Prog. Photovolt., Res. Appl.* **22** 277–82
- [5] Kupec J, Stoop R L and Witzigmann B 2010 Light absorption and emission in nanowire array solar cells *Opt. Express* **18** 27589–605
- [6] Fukui T, Yoshimura M, Nakai E and Tomioka K 2012 Position-controlled III–V compound semiconductor nanowire solar cells by selective-area metal–organic vapor phase epitaxy *Ambio* **41** 119–24
- [7] Wallentin J et al 2013 InP nanowire array solar cells achieving 13.8% efficiency by exceeding the ray optics limit *Science* **339** 1057–60
- [8] Åberg I et al 2016 A GaAs nanowire array solar cell with 15.3% efficiency at 1 sun *IEEE J. Photovolt.* **6** 185–90
- [9] Van Dam D, Van Hoof N J J, Cui Y, Van Veldhoven P J, Bakkers E P A M, Gómez Rivas J and Haverkort J E M 2016 High-efficiency nanowire solar cells with omnidirectionally enhanced absorption due to self-aligned indium-tin-oxide mie scatterers *ACS Nano* **10** 11414–9
- [10] Yazawa M, Koguchi M, Muto A, Ozawa M and Hiruma K 1992 Effect of one monolayer of surface gold atoms on the epitaxial growth of InAs nanowhiskers *Appl. Phys. Lett.* **61** 2051–3
- [11] Haraguchi K, Katsuyama T and Hiruma K 1994 Polarization dependence of light emitted from GaAs p-n junctions in quantum wire crystals *J. Appl. Phys.* **75** 4220–5
- [12] Koguchi M et al 2002 Growth and optical properties of nanometer-scale GaAs and InAs whiskers *J. Appl. Phys.* **77** 447–62
- [13] Pellegrino S and Tarricone L 2000 MOVPE growth and study of InP-based materials: opportunities and challenges *Mater. Chem. Phys.* **66** 189–96
- [14] Duan X and Lieber C M 2000 General synthesis of compound semiconductor nanowires *Adv. Mater.* **12** 298–302
- [15] Samuelson L, Magnusson M H, Deppert K and Heurlin M 2016 Gas-phase synthesis method for forming semiconductor nanowires US PATENT 9447520B2 87 021001
- [16] Heurlin M, Magnusson M H, Lindgren D, Ek M, Wallenberg L R, Deppert K and Samuelson L 2012 Continuous gas-phase synthesis of nanowires with tunable properties *Nature* **492** 90–94
- [17] Wagner R S and Ellis W C 1964 Vapor-liquid-solid mechanism of single crystal growth *Appl. Phys. Lett.* **4** 89–90
- [18] Schmidt V, Wittmann J V, Senz S and Gösele U 2009 Silicon nanowires: a review on aspects of their growth and their electrical properties *Adv. Mater.* **21** 2681–702
- [19] Persson A I, Larsson M W, Stenström S, Ohlsson B J, Samuelson L and Wallenberg L R 2004 Solid-phase diffusion mechanism for GaAs nanowire growth *Nat. Mater.* **3** 677–81
- [20] Deppert K, Bovin J-O, Malm J-O and Samuelson L 1996 A new method to fabricate size-selected compound semiconductor nanocrystals: aerotaxy *J. Cryst. Growth* **169** 13–19
- [21] Deppert K, Bovin J-O, Magnusson M H, Malm J-O, Svensson C and Samuelson L 1999 Aerosol fabrication of nanocrystals of InP *Jpn. J. Appl. Phys.* **38** 1056–9
- [22] Turkevich J, Stevenson P C and Hillier J 1951 A study of the nucleation and growth processes in the synthesis of colloidal gold *Discuss. Faraday Soc.* **11** 55–75
- [23] Brust M, Walker M, Bethell D, Schiffrin D J and Whyman R 1994 Synthesis of thiol-derivatised gold nanoparticles in a two-phase liquid-liquid system *J. Chem. Soc. Chem. Commun.* **1994** 801–2
- [24] Mafuné F, Kohno J, Takeda Y, Kondow T and Sawabe H 2001 Formation of gold nanoparticles by laser ablation in aqueous solution of surfactant *J. Phys. Chem. B* **105** 5114–20
- [25] Ahmad T, Wani I A, Lone I H, Ganguly A, Manzoor N, Ahmad A, Ahmed J and Al-Shihri A S 2013 Antifungal activity of gold nanoparticles prepared by solvothermal method *Mater. Res. Bull.* **48** 12–20
- [26] Ma H, Yin B, Wang S, Jiao Y, Pan W, Huang S, Chen S and Meng F 2004 Synthesis of silver and gold nanoparticles by a novel electrochemical method *ChemPhysChem* **5** 68–75
- [27] Magnusson M H, Ohlsson B J, Björk M T, Dick K A, Borgström M T, Deppert K and Samuelson L 2014 Semiconductor nanostructures enabled by aerosol technology *Front. Phys.* **9** 398–418

- [28] Dubrovskii V G 2015 Theory of VLS growth of compound semiconductors *Semiconductors and Semimetals* (Waltham: Academic) pp 1–78
- [29] Jindal V and Shahedipour-Sandvik F 2009 Theoretical prediction of GaN nanostructure equilibrium and nonequilibrium shapes *J. Appl. Phys.* **106** 083115
- [30] Magnusson M H, Deppert K, Malm J O, Bovin J O and Samuelson L 1999 Gold nanoparticles: production, reshaping, and thermal charging *J. Nanoparticle Res.* **1** 243–51
- [31] Karlsson M N A, Deppert K, Karlsson L S, Magnusson M H, Malm J O and Srinivasan N S 2005 Compaction of agglomerates of aerosol nanoparticles: a compilation of experimental data *J. Nanoparticle Res.* **7** 43–49
- [32] Gudiksen M S, Wang J and Lieber C M 2002 Size-dependent photoluminescence from single indium phosphide nanowires *J. Phys. Chem. B* **106** 4036–9
- [33] Hou J J, Wang F, Han N, Zhu H, Fok K, Lam W, Yip S, Hung T, Lee J E Y and Ho J C 2013 Diameter dependence of electron mobility in InGaAs nanowires *Appl. Phys. Lett.* **102** 093112
- [34] Alcott G, Magnusson M, Postel O, Deppert K, Samuelson L and Ohlsson J 2017 Concentric flow reactor US PATENT 9574286 B2
- [35] Barrigón E, Hultin O, Lindgren D, Yadegari F, Magnusson M H, Samuelson L, Johansson L I M and Björk M T 2018 GaAs nanowire pn-junctions produced by low-cost and high-throughput Aerotaxy *Nano Lett.* **18** 1088–92
- [36] Preger C, Overgaard N C, Messing M E and Magnusson M H 2020 Predicting the deposition spot radius and the nanoparticle concentration distribution in an electrostatic precipitator *Aerosol Sci. Technol.* **54** 718–28
- [37] Kobayashi N P, Logeeswaran V J, Li X, Islam M S, Straznicky J, Wang S-Y and Williams R S 2007 Randomly oriented indium phosphide nanowires for optoelectronics *Nanophotonics for Communication: Materials, Devices, and Systems IV* vol 6779 p 67790E
- [38] Pignatola P, Lee H, Qiao L, Tseng M and Yi Y 2011 Graded index and randomly oriented core-shell silicon nanowires for broadband and wide angle antireflection *AIP Adv.* **1** 032124
- [39] Naseem U and Kunze K 2020 Shell-enabled vertical alignment and precision-assembly of a close-packed colloidal crystal film US PATENT 20170358448A1
- [40] Metaferia W et al 2016 GaAsP nanowires grown by Aerotaxy *Nano Lett.* **16** 5701–7
- [41] Metaferia W, Sivakumar S, Persson A R, Geijselaers I, Wallenberg L R, Deppert K, Samuelson L and Magnusson M H 2018 N-type doping and morphology of GaAs nanowires in Aerotaxy *Nanotechnology* **29** 285601
- [42] Persson A R, Metaferia W, Sivakumar S, Samuelson L, Magnusson M H and Wallenberg R 2018 Electron tomography reveals the droplet covered surface structure of nanowires grown by Aerotaxy *Small* **14** 1801285
- [43] Caroff P, Bolinsson J and Johansson J 2011 Crystal phases in III-V nanowires: from random toward engineered polytypism *IEEE J. Sel. Top. Quantum Electron.* **17** 829–46
- [44] Yang F, Messing M E, Mergenthaler K, Ghasemi M, Johansson J, Wallenberg L R, Pistol M, Deppert K, Samuelson L and Magnusson M H 2015 Zn-doping of GaAs nanowires grown by Aerotaxy *J. Cryst. Growth* **414** 181–6
- [45] Sun W, Guo Y, Xu H, Gao Q, Hoe Tan H, Jagadish C and Zou J 2013 Polarity driven simultaneous growth of free-standing and lateral GaAsP epitaxial nanowires on GaAs (001) substrate *Appl. Phys. Lett.* **103** 223104
- [46] Johansson J, Ghasemi M, Sivakumar S, Persson A R, Metaferia W and Magnusson M H 2020 Understanding Zn doping of GaAs nanowires (in preparation)
- [47] Johansson J, Svensson C P T, Mårtensson T, Samuelson L and Seifert W 2005 Mass transport model for semiconductor nanowire growth *J. Phys. Chem. B* **109** 13567–71
- [48] Dubrovskii V G, Berdnikov Y, Schmidtbauer J, Borg M, Storm K, Deppert K and Johansson J 2016 Length distributions of nanowires growing by surface diffusion *Cryst. Growth Des.* **16** 2167–72
- [49] Johansson J and Magnusson M H 2019 From diffusion limited to incorporation limited growth of nanowires *J. Cryst. Growth* **525** 125192
- [50] COMSOL Multiphysics® v. 5.4 COMSOL AB, Stockholm, Sweden (available at: www.comsol.com)